Available online at www.sciencedirect.com

ScienceDirect

Geochimica et Cosmochimica Acta 188 (2016) 106–124

Geochimica et Cosmochimica Acta

www.elsevier.com/locate/gca

The CO chondrites: Major recent Antarctic finds, their thermal and radiation history, and describing the metamorphic history of members of the class

Derek W.G. Sears

Bay Area Environmental Research Institute/NASA Ames Research Center, Space Science and Astrobiology Division (MS 245-3), Mountain View, CA 94035, USA

Received 22 December 2015; accepted in revised form 19 May 2016; available online 28 May 2016

Abstract

Thermoluminescence (TL) properties of 29 CO chondrites from the Miller Range (MIL) and five chondrites from the Dominion Range (DOM) have been measured. MIL has a relatively strong natural TL signal (19.6 ± 14.7 krad), while some of the DOM samples have a very weak natural TL signal (<1 krad) whereas others resemble the MIL meteorites. I argue that MIL and some of the DOM samples had a normal perihelion (∼1.0 AU) and terrestrial age of ∼450–700 ka, while some of the DOM samples have a terrestrial age of ∼100 ka but a perihelion of ∼0.8 AU. The DOM meteorites also show considerable heterogeneity in their induced TL properties, also suggesting that the DOM fragments represent more than one fall. The induced TL data for the MIL samples studied here are consistent with them all being from a single fragmented meteorite. Small (50 mg) chips have TL properties similar to 500 mg chips, so that the smaller chips are representative, although samples taken from original masses less than ∼2 g have low natural TL suggesting that they were heated during atmospheric fall. The properties of CO chondrites are reviewed in terms of their petrologic types. Correlations between TL sensitivity, the most quantitative technique for evaluating metamorphic alteration in CO chondrites, and data for olivine composition and heterogeneity, matrix composition, inert gas content, metal composition (Ni, Co, and Cr in the kamacite), bulk carbon, C and O isotopes, graphite ordering, spectral reflectance at 0.8 μm, and textural characteristics of the ameboid olivine and Ca-rich inclusions are examined. The petrographic types appear to be largely metamorphic in origin with perhaps a minor role for metasomatism. Contrary to recent proposals it is here argued that petrologic type definitions should (1) be specific enough to be meaningful, but broad enough to be simple in application and robust to new developments, (2) be descriptive and not interpretative, (3) should not oversimplify and obscure important class-to-class differences, and (4) take account of all the available information, while avoiding reliance on any one technique or single observation whose application is based on interpretation. With these considerations in mind the petrographic type definitions for CO chondrites are restated and the petrologic type of 3.2 assigned to both the MIL and DOM CO chondrites.

Keywords: CO chondrites; Metamorphism; Thermoluminescence; Antarctic meteorites

1. INTRODUCTION

The CO chondrites are a group of six observed falls and 459 finds (Table 1). Of the 459 finds, 283 were found in the Antarctic and of these, 204 were found at the Miller Range (83°15′S 157°00′E) and 11 were found at the Dominion Range (85°20′S 166°30′E). The Antarctic meteorite program has resulted in the recovery of large numbers of especially important meteorites, including lunar meteorites, martian meteorites and meteorites of low petrographic type such as these CO chondrites (Cassidy et al., 1992). However, since meteorites fragment in the atmosphere, and on

http://dx.doi.org/10.1016/j.gca.2016.05.033
0016-7037/

Table 1
Statistics for the known CO chondrites.*

Observed falls				World-wide finds		Antarctic finds	
Meteorite	Year	Location	Mass	Country/region	No.	Region/icefield	No.
Ornans	1868	Franche-Comte, France	6 kg	Algeria	7	Allan Hills	7
Lancé	1872	Centre, France	51.7 kg	Antarctica	283	Asuka	9
Warrenton	1877	Missouri, USA	1.6 kg	Australia	2	Buckley Island	1
Felix	1900	Alabama, USA	3.2 kg	Chile	6	Dominion Range	11
Kainsaz	1937	Tatarstan, Russia	200 kg	Egypt	1	Elephant Moraine	3
Moss	2006	Ostfold, Norway	3.76 kg	Lybia	51	Frontier Mountains	2
				Morocco	15	Graves Nunatak	1
				Niger	1	Grove Mountains	1
				Northwest Africa	78	LaPaz Icefield	2
				Oman	6	Larkman Nunatak	2
				Sahara	5	Meteorite Hills	3
				Saudi Arabia	2	Miller Range	204
				USA	2	Queen Alexandra Range	1
				Total	459	Szabo Bluff	2
						Yamato	34
						Total	283

* Data from the Meteoritical Society database (www.lpi.usra.edu/meteor/) as of October 2014.

the ground, the number of discrete finds represented among the 459 individual meteorite fragments is unknown, and maybe only a few individual meteorites are present in this population. With only six observed falls, there has been an uncomfortable dependence on the finds for CO chondrite studies, despite the sometimes major weathering processes the finds have suffered and the sensitivity of many physical and compositional parameters to weathering. Nevertheless, the MIL and DOM meteorites represent a major fraction of the total CO chondrite material available to science and are worthy of closer attention. In fact, if most or all of the Miller Range and Dominion Range are fragments of single major falls at each site, as suggested in the Antarctic Meteorite Newsletter, these paired meteorite finds also offer an opportunity to explore the heterogeneity and brecciation of two especially large meteorites.

Since "pairing" (identifying fragments that belonged to a single meteorite) is such a problem among the Antarctic meteorite finds, and members of most meteorite classes look so similar, it is helpful to identify physical means by which members of a single fall might be identified. Two examples of such means are terrestrial age and orbit, although of course these also have scientific value in their own right. Techniques available for determining the terrestrial age of Antarctic meteorites include the measurement of cosmogenic isotopes (e.g. Nishiizumi et al., 1979; Jull et al., 1998) and natural thermoluminescence (Melcher, 1981a; Benoit et al., 1993). Orbits cannot easily be determined from the recovered meteorites, although natural thermoluminescence can provide some indication of the orbital perihelion (Melcher, 1981b; Benoit and Sears, 1997).

The best recent review of geological properties of the CO chondrites is probably that of Cloutis et al. (2012). The CO chondrites have major element composition that puts them among the carbonaceous chondrite groups (along with the CI, CM, CV, and CR classes), but with minor and trace element compositions and mineralogical, petrographic and isotopic properties that set them apart from the others and into the CO group (McSween, 1979; Kallemeyn and Wasson, 1981; Zolensky et al., 1993; Brearley and Jones, 1998). They are ~45 vol% chondrules (which are relatively small, ~0.15 mm), 40 vol% matrix, ~10 vol% refractory inclusions, and ~5 vol% metal and sulfide. They contain little, if any, phyllosilicates but instead contain the major anhydrous minerals olivine and pyroxene with feldspathic components primarily as chondrule mesostasis. The CO chondrites are type 3 in the Van Schmus and Wood (1967) scheme, meaning that they have heterogeneous mineral compositions, sharp textures, and relatively high contents of volatile constituents reflecting relatively little parent body metamorphism relative to, say, the equilibrated ordinary chondrites. Notwithstanding differences in elemental and isotopic bulk composition, the CO chondrites are mineralogically and petrographically similar to unequilibrated (type 3) ordinary chondrites.

Probably the CO chondrite feature that has attracted most attention is that, like the ordinary chondrites the CO chondrites reflect a range of alteration by metamorphism (and possibly metasomatism) on their parent asteroid (Wood, 1962; Van Schmus and Wood, 1967; Sears et al., 1980). This was described by McSween (1979) who sorted the CO chondrites into three metamorphic groups on the basis of olivine and pyroxene composition, metal composition, chondrule texture, matrix composition and volatiles. Scott and Jones (1990) revisited the issue and, using similar data plus TL sensitivity (Keck and Sears, 1987), recast the meteorites into petrologic types 3.0–3.9 in a manner analogous to the scheme previously devised for type 3 ordinary chondrites (Sears et al., 1980). Sears et al. (1991) added further meteorites, folded-in cathodoluminescence observations, and concurred with the Scott and Jones scheme while making minor revisions to the placement of a few individual meteorites. Initial examination of the Miller Range and Dominion Range CO chondrite finds in the Antarctic Meteorite Newsletter indicated that they were of petrographic type 3.2.

The refractory inclusions have also been examined for evidence of metamorphic alteration. Russell et al. (1998) examined the CAI in a suite of CO3 chondrites and recorded a number of changes. As metamorphism reached type 3.4 levels, spinel became Fe rich (50–60 mol%) and perovskite was converted to ilmenite. Melilite inclusions, that were abundant in petrologic types 3.0–3.3, were rare in type 3.4, and absent in types 3.5–3.7. Above type 3.7, the magnesium–aluminum systematics were severely disturbed. Chizmadia et al. (2002) have shown that the ameboid olivine inclusions show the effects of metamorphic alteration. The thickness of ferroan olivine veins and the thickness of halos around the forsteritic cores increase with increasing metamorphism and these authors identified these changes with specific petrologic types. The TL properties of refractory inclusions in CO chondrites have never been studied, but Guimon et al. (1995) examined the TL properties of CAI from Allende CV3 chondrite and found that these metamorphism-driven mineralogical changes in mineralogy were reflected in the induced TL properties of the inclusions.

An additional parameter was added to the armory of data to describe metamorphic alteration in CO chondrites by Bonal et al. (2007) who showed that the graphitization (or ordering) of the amorphous carbon increased with metamorphism. They proposed a complete revision of the petrologic type definitions for CO chondrites in an attempt to devise a scheme that could be applied across the meteorite classes.

Most recently, the prospect of using remote sensing techniques to identify the petrologic types of CO-like asteroids has been explored by Cloutis et al. (2012). Spectral reflectivity of the CO chondrites reflects metamorphic changes since it is sensitive to the changes in the mineralogy of the meteorites. The major quantitative parameter to emerge from the Cloutis et al. (2012) study is the reflectance at 0.8 μm. This is the second example of spectral reflectivity data being used to determine petrologic type remotely, the first being the use of clinopyroxene/orthopyroxene ratio in ordinary chondrites which decreases with petrologic type and can be detected remotely for asteroids using reflectivity spectra (Gietzen et al., 2012).

On the oxygen three-isotope diagram, the type 3 ordinary chondrites are displaced from the equilibrated ordinary chondrites along a mass fractionation line (Clayton et al., 1991) and to some extent petrologic type differences among the type 3 ordinary chondrites can be observed in $\delta^{18}O$ (Sears and Weeks, 1983). Greenwood and Franchi (2004) investigated this for CO chondrites and found subtle increase in $\Delta^{17}O$ values with increasing metamorphic grade for types 3.1–3.4, which did not persist at higher types, and they found $\Delta^{13}C$ values of CO3 falls decrease with increasing metamorphic grade. However, there are some concerning discrepancies between their data and that of Clayton and Mayeda (1999) which show a steady increase in $\delta^{18}O$ with petrologic type.

Greenwood and Franchi (2004) emphasized the major influence of weathering on C and O isotopes and cautioned the use of data obtained from finds. The subject was more broadly reviewed by Bland et al. (2006) who state that C chondrites are especially vulnerable to weathering effects. It seems that most or all of the parameters used to determine petrologic types could be affected by weathering, some more than others, and in some cases it may be difficult to detect or correct for. This is unfortunate because with the number of observed CO3 chondrite falls being so few, and the available observed falls being largely in the center of the metamorphic range, much of our understanding of this class is based on finds. Since some caution is needed for assigning petrologic types to CO chondrite because so many are finds, it becomes particularly desirable not to rely on any one technique, but look for consensus among the various techniques.

This paper reports thermoluminescence (TL) measurements on 29 CO3 chondrites from Miller Range and five CO3 chondrites from Dominion Range. The CO chondrites from Miller Range, and to some extent Dominion Range, are important and worthy of special attention for two major reasons. (1) They are an especially low petrologic type and therefore retain memories of the pre-accretionary, solar nebular, properties. The published type assignments were made in survey mode using only optical microscopy and electron microprobe analysis. (2) The sheer mass (almost 18 kg in the case of Miller Range) mean that a large amount of low petrologic type CO chondrite material is available for research and the better understanding we have of this material, not just its petrologic type but its physical history, the greater benefit will accrue. I discuss their weathering, their terrestrial age, and the perihelia of their orbits, and how these data confirm the proposed pairing for these meteorites, and I discuss their heterogeneity and brecciation, and their petrographic type and thus how close to their original (i.e. premetamorphic) state they are. This study was the subject of an earlier progress report (Sears, 2013), which is superseded by the present paper. I also use this opportunity to record some notes on the petrographic type definitions for CO3 chondrites in the light of the new data, newly available parameters, and recent discussions in the literature. Combining data on these new CO chondrites with a discussion of their petrologic types is important, other than to avoid needless propagation of papers and increased workloads, since I wanted to remove ambiguity and confusion recently introduced in the literature prior to publishing my suggested types for these two important CO chondrite finds.

2. EXPERIMENTAL

Duplicate chips of the CO3 chondrites listed in Table 2 were obtained from the Meteorite Processing Laboratory at the Johnson Space Center. Originally 50 mg chips were requested, so as to maximize the likelihood of sampling unusual inclusions and fully assess the level of homogeneity. However, when the study of these was complete it was found helpful to compare the results with data from 500 mg chips for selected samples. With one exception, our procedures are the same as used in previous natural and induced thermoluminescence (TL) studies at the University of Arkansas that were recently summarized by Sears et al. (2013). The exception is that in order to have

Table 2
Natural TL data (krad) for Dominion Range (DOM and Miller Range (MIL) CO3 chondrites.*

Meteorite	Parent Mass (g)	LT/HT_1	LT/HT_2	LT/HT_{mean}	NTL
DOM pairing group					
50 mg samples					
DOM 08139,6 and 7	21.8	1.35	1.27	1.31	19.7
DOM 10104,8 and 9	201	1.16	2.2	1.68	27.1
DOM 10121,6 and 7	16.2	0.22	0.18	0.18	1.73
DOM 10299,6 and 7	14.8	0.22	0.2	0.20	1.85
DOM 10900,5 and 6	26.1	0.1	–	0.10	<1
500 mg samples					
DOM10104,18 and 19	201	1.74	0.74	1.24	18.3
DOM10900, 9 and 10	26.1	–	–	–	<1
MIL pairing group					
50 mg samples					
MIL 07099,5 and 6	13.08	0.78	0.95	0.87	11.5
MIL 07182,5 and 6	111.98	1.3	1.25	1.28	19.0
MIL 07193,6 and 7	14.96	1.25	1.73	1.49	23.2
MIL 07293,6 and 7	15.33	1.02	1.12	1.07	15.2
MIL 07341,6 and 7	32.02	1.6	2.7	2.15	37.3
MIL 07342,6	31.354	1.04	–	1.04	14.6
MIL 07346,6 and 7	39.671	1.22	1.06	1.14	16.4
MIL 07384,5 and 6	28.602	1.15	4.5	2.83	53.1
MIL 07459,7 and 8	18.331	1.11	0.82	0.97	13.3
MIL 090019, 6 and 7	793.8	1.5	1.4	1.45	22.4
MIL 090073, 6 and 7	255.5	1.03	3.53	2.28	40.3
MIL 090152,6 and 7	40.36	1.17	1.34	1.26	18.6
MIL 090227,6 and 7	62.81	1.56	1.6	1.58	25.1
MIL 090480,6 and 7	65.418	1.4	1.79	1.60	25.4
MIL 090543,3 and 4	4.79	1.4	1.4	1.40	21.4
MIL 090705,4 and 5	4.86	1.37	1.04	1.21	17.7
MIL 090785,8 and 9	90.34	4.4	2.42	3.41	67.7
MIL 090821,5 and 6	1.3	0.3	0.18	0.24	2.2
MIL 090891,3 and 5	6.95	nd	0.65	0.65	8.0
MIL 090897,3 and 4	2.51	1.2	1.3	1.25	18.5
MIL 090907,3 and 4	1.78	0.63	1.02	0.83	10.8
MIL 090915,4 and 5	7.342	1.2	1.1	1.15	16.6
MIL 090919,4 and 5	3.865	1.0	1.1	1.05	14.8
MIL 090983,4 and 5	1.46	0.09	0.17	0.13	<1
MIL 090988,4 and 5	3.84	>0.63	1.21	1.21	17.8
MIL 090989,4 and 5	2.09	0.33	0.89	0.61	7.3
500 mg samples					
MIL 07182,11 and 12	111.98	1.7	0.92	1.31	19.7
MIL 090019,9 and 10	793.8	1.48	1.71	1.60	25.4

* Masses quoted are the original mass of the parent meteorite, taken from the Antarctic Meteorite database (http://curator.jsc.nasa.gov/antmet/us_clctn.cfm) in October 2014. The significant figures quoted are as given in the database. Natural TL data were not obtained for three samples MIL 090293, 090890, and 090067, because of laboratory mishaps. LT/HT(1) and LT/HT(2) refer to the ratio of the low temperature TL (~250 °C) to the high temperature TL (~400 °C) for the two chips. NTL is calculated from the mean LT/HT by the methods of Hasan et al. (1989).

a meaningful number of samples I waived our previous requirement that the mass of the original parent sample had to be greater than 20 g. We continued to require that samples were taken at least 6 mm from any potential fusion crust to avoid the effects of atmospheric heating on the natural TL (Sears, 1975), but this criterion may sometimes have been violated. Recall that the radius of 2, 5, 10 and 20 g spheres of with the density of chondrites are 0.5, 0.7, 0.9, and 1.2 cm, respectively. Chips were selected so as to represent different lithologies when present; however, in general the duplicate chips appeared fairly uniform because of staining by weathering. Similarly, anomalous inclusions inside the chips will have been missed and will not affect the appearance of the ground powders because of homogenization and dispersal of weathering products. Working in red light, to avoid any fading that might be caused by fluorescent lighting, the samples were gently crushed in a stainless mortar and pestle, the metal removed with a hand magnet, and then the non-magnetic portion gently crushed again to about 200 μm in an agate mortar and pestle. Before and after crushing the powders were viewed under a binocular microscope to check for unusual inclusions, evidence for fusion crust or any obvious weathering products.

A four-mg aliquot from each fragment was placed in a 5 mm diameter copper pan for measurement in a modified Daybreak Nuclear and Medical Inc. TL reader. This is a commercial instrument that have modified to (1) place the sample nearer the detector (an EMI 9635QB photomultiplier tube), (2) screen off black body from the heating strip using a 4 mm copper aperture, a blue filter, and a heat filter, and (3) enable the PMT to remain on permanently by installation of a shutter, which improves stability.

The TL is measured in the blue-green region between room temperature and 500 °C, with a heating rate of 7.5°/s. The plot of light emitted as a function of laboratory heating temperature is referred to as the "glow curve" (Garlick, 1949). After measurement of the TL for the "as-received" sample (which I will refer to as the natural TL) the copper pan with the sample was placed in a radiation cell that exposed it to a 145 mCi ^{90}Sr source for 3 min. The sample was then returned to the TL rig and thus the TL induced measured again. This was repeated a further two times. After the last measurement, the sample was heated once more and the background and black-body radiation was recorded.

The record for each sample therefore consists of five glow curves, one for the sample in its natural state, three for the sample in its irradiated state, and one to record the background and black-body. At the beginning of each day, a sample of the Dhajala H3.8 chondrite, prepared in the same way as the present meteorite samples, was run as a normalization standard and long-term stability check for the apparatus.

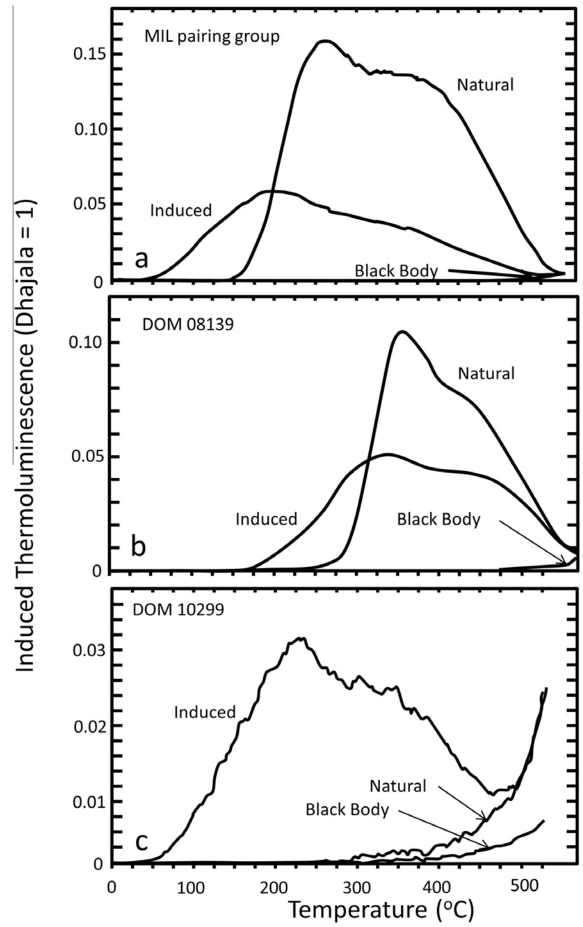

Fig. 1. Representative glow curves (plots of light emitted as a function of laboratory heating temperature) for three representative CO chondrites in the present study. Both the natural TL and induced TL curves are shown. Natural TL is the "as received" signal, induced TL is the signal after removal of the natural TL and exposure to a dose of radiation from a ^{90}Sr β-source. Additionally, the background/black body curve is shown, which is the signal observed after the natural and induced TL have been removed by a short heating to 500 °C. The meteorites from the Dominion Range showed two kinds of curves. (a) The MIL group show a strong natural signal peaking at about 250 °C with a secondary peak at ~400 °C. The induced glow curve consisted of a broad band beginning at about 100 °C, peaking at ~200 °C, and continuing to ~400 °C. (b) DOM 08139 showed strong natural peaks at 300 °C with a weaker peak at ~400 °C and induced TL that started at about 200 °C, peaked at ~300 °C and showed other peaks at ~450 °C. (c) DOM10299 showed little natural TL (half the signal at 450 °C was due to black body radiation) and weak induced TL starting at about 100 °C, peaking at about 200 °C, and continuing until about 400 °C.

3. RESULTS

Examples of the glow curves produced by the present samples are shown in Fig. 1. I observed essentially one kind of behavior for the Miller range meteorites (Fig. 1a) and two for the Dominion Range meteorites (Fig. 1b and c). The MIL samples all produced curves with a strong natural signal peaking at about 250 °C with a secondary peak at ~400 °C. The induced glow curve consisted of a broad band beginning at about 100 °C, peaking at ~200 °C, and continuing to ~400 °C. Black body was insignificant in this case because the TL signals were so strong.

Two of the DOM samples, DOM10104 and DOM08139 (Fig. 1b), showed strong natural peaks 300 °C with a weaker peak at ~400 °C and induced TL that started at about 200 °C, peaked at ~300 °C and showed other peaks at ~450 °C. One split from DOM 10121 had a curve quite unlike bulk CO samples but very similar to EGG4 in the study of Allende CAIs by Guimon et al. (1995). I conclude that despite our care in sampling, the small size of refractory inclusions in CO chondrites and weather staining of the samples meant that a refractory inclusion had compromised the data for this split and it will not be discussed further in this paper. The second split of DOM 10121 and the two remaining DOM samples, DOM10900 and DOM10299 (Fig. 1c), showed little natural TL and the natural TL that was present did not start appearing until >300 °C and half the signal at 450 °C was due to black body. These two samples had weak induced TL starting at about 100 °C, peaking at about 200 °C, and continuing until about 400 °C and, again, black body was significant

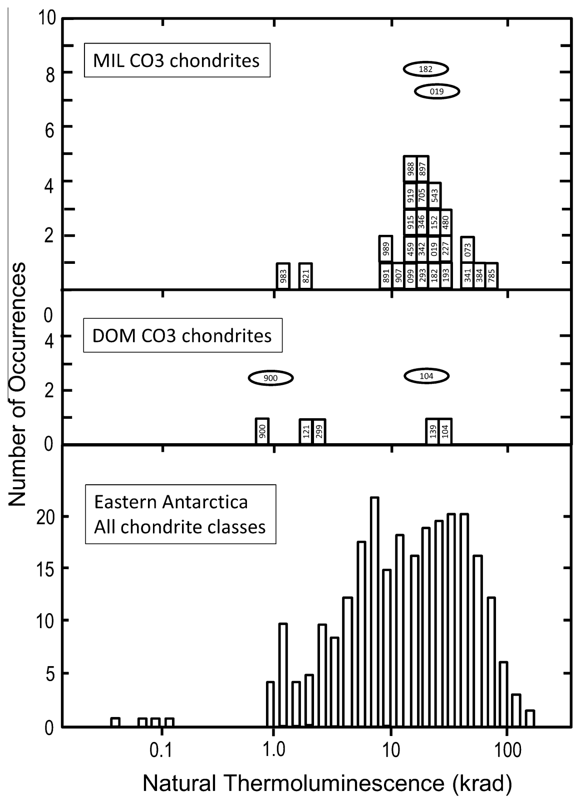

Fig. 2. Histograms of the natural TL of the present CO chondrites compared with a compilation of data for meteorites recovered from eastern Antarctica. The MIL meteorites show a single tight cluster at ~20 krad while the DOM meteorites are bimodal with some at ~20 krad and as many at ~1.0 krad. By contrast, the asymmetric distribution (on a log scale), which peaks at ~50 krad, drops off rapidly to higher values (reaching ~200 krad), and drops off slowly to lower values (reaching ~0.1 krad). The compilation of data is from Sears et al. (2013).

at high temperatures. For quantitative measurements black body must be subtracted in these cases.

I calculated the natural TL data in terms of absorbed dose (in krad) using the methods of Hasan et al. (1989), namely the natural $TL = \exp(2.303 \times (\log(LT/HT) + 0.884)/0.775)$. (The SI unit for absorbed dose is the Gray, where 1 krad = 10 Gray, but krad are used here to be consistent with earlier publications). The data are shown in Fig. 2 and listed in Table 2. The natural TL data for Miller Range show a strong peak in the histogram at ~20 krad with relatively little scatter. The two 500 mg samples showed behavior in good agreement with the data for the 50 mg chip which suggests that 50 mg chips of these meteorites are representative. Only two samples fall more than two sigma from the mean, MIL090821,5 and 6, and MIL090983,4 and 5, and without these the average and standard deviation of 25 samples is 14.4 ± 6.5 krad. The most likely explanations for the outliers are that either (1) these samples were all taken too close to the fusion crust, despite duplicate chips being taken, or (2) the original meteorite was so small that it was impossible to sample material that had not been heated during atmospheric passage. These problems were anticipated in the Section 2. DOM08139 and DOM10104 have natural TL values also ~15 krad while the other DOM samples are <1.0 krad. The reason for this spread in data might be that there are two separate meteorite falls in this database. Thus the lower samples were either taken too close to the fusion crust, again despite good agreement between duplicate chips, or that the sample was too small for its interior to escape atmospheric heating. Fig. 2 also shows, for comparison, a compilation of the natural TL for meteorites from the eastern Antarctic. The CO chondrites under study here plot in the center of the logarithmic range observed for Antarctic meteorites.

The induced TL data are shown in Tables 3and 4. Two parameters are reported; TL peak temperatures (usually there are three peaks in each glow curve) and TL sensitivity for each peak or inflection. Fig. 3 shows the positions of the apparent peaks in these CO chondrite glow curves. Clearly several TL peaks are present in these CO chondrite glow curves. Even in the absence of a peak or inflection, additional peaks can be inferred from an abnormally wide peak although these are not included in the reported data. Despite these complications and the resulting scatter, especially for the highest temperature peak, in these low petrographic type meteorites it is clear that there are three dominant peaks, at ~120 °C, ~200 °C, and ~300 °C. Also shown in Fig. 3 are data for the 500 mg chips which are in agreement with the data for 50 mg chips but for obvious reasons plot closer to the averages.

The TL sensitivities for these three peaks as observed in the Miller Range meteorites are shown in Fig. 4. Peak 1 values center on a value of ~0.046, while peak 2 centers on ~0.18 and peak 3 centers on ~0.10, although there is a suggestion of bimodality with values at ~0.068 and ~0.14 for peak 3. MIL 090073 and MIL 090983 values below 0.01. Also shown are TL sensitivities for the 500 mg samples of two of the MIL chips, MIL 090019 and MIL 07182. In all cases, the data for the 500 mg samples are in reasonable agreement with the peak in the histograms.

The TL sensitivities for the three induced TL peaks as observed in the Dominion Range meteorites are shown in Fig. 5. The TL sensitivity data for these few meteorites do not show preferred values. The two chips from DOM 08139 and DOM 10104 have values of ~0.19, ~0.31, ~0.35 for peak 1, peak 2 and peak 3, respectively, while the other meteorites have values at or below 0.1. This difference in the TL sensitivities of the 50 mg chips was borne out by the data for the 500 mg chips of DOM 10900 and DOM 10104 which confirm the almost factor 100 difference in TL sensitivity.

4. DISCUSSION

The TL measurements of the samples in the present study clearly demonstrate the precision and reproducibility of such measurements when applied to meteorites. They show that, in general, peak temperatures and intensities are within the limits that have been published over several decades. Not-with-standing this, these data also reflect the difficulties faced by any technique that attempts to extract

Table 3
Induced thermoluminescence data for Miller Range (MIL) CO3 chondrite samples.*

Meteorite	Parent	Peak 1		Peak 2		Peak 3	
	Mass (g)	Peak T (°C)	TL sensitivity (Dhajala = 1)	Peak T (°C)	TL sensitivity (Dhajala = 1)	Peak T (°C)	TL sensitivity (Dhajala = 1)
50 mg samples							
MIL 07099,5	13.08	152 ± 12	0.100 ± 0.003	204 ± 9	0.129 ± 0.005	325 ± 13	0.081 ± 0.010
MIL 07099,6		127 ± 16	0.043 ± 0.004	204 ± 7	0.092 ± 0.009	333 ± 10	0.071 ± 0.007
MIL 07182,5	111.98	–	–	219 ± 7	0.347 ± 0.035	305 ± 10	0.049 ± 0.005
MIL 07182,6		123 ± 4	0.106 ± 0.030	224 ± 5	0.359 ± 0.070	–	0.000 ± 0.000
MIL 07193,6	14.96	–	–	202 ± 3	0.081 ± 0.018	298 ± 9	0.063 ± 0.010
MIL 07293,6	15.33	129 ± 4	0.054 ± 0.007	201 ± 3	0.143 ± 0.021	271 ± 7	0.100 ± 0.017
MIL 07293,7		129 ± 5	0.062 ± 0.005	194 ± 4	0.139 ± 0.011	270 ± 10	0.095 ± 0.012
MIL 07341,6	32.02	119 ± 12	0.000 ± 0.000	200 ± 6	0.154 ± 0.009	319 ± 53	0.107 ± 0.008
MIL 07341,7		125 ± 13	0.067 ± 0.007	200 ± 20	0.119 ± 0.012	306 ± 31	0.073 ± 0.007
MIL 07342,6	31.354	117 ± 7	0.092 ± 0.008	189 ± 10	0.161 ± 0.009	312 ± 13	0.110 ± 0.004
MIL 07346,6	39.671	–	0.000 ± 0.000	219 ± 7	0.168 ± 0.008	331 ± 33	0.134 ± 0.010
MIL 07346,7		117 ± 14	0.085 ± 0.021	321 ± 32	0.239 ± 0.031	302 ± 4	0.223 ± 0.029
MIL 07384,5	28.602	138 ± 2	0.107 ± 0.020	181 ± 7	0.127 ± 0.020	313 ± 13	0.082 ± 0.019
MIL 07384,6		–	–	178 ± 6	0.690 ± 0.065	–	–
MIL 07459,15	18.331	130 ± 5	0.035 ± 0.002	208 ± 3	0.066 ± 0.003	300 ± 30	0.047 ± 0.006
MIL 07459,7		133 ± 3	0.058 ± 0.003	213 ± 3	0.108 ± 0.010	332 ± 14	0.058 ± 0.008
MIL 090019,6	793.800	–	–	190 ± 4	0.062 ± 0.011	312 ± 16	0.040 ± 0.009
MIL 090019,7		–	–	210 ± 4	0.157 ± 0.029	296 ± 14	0.136 ± 0.024
MIL 090073, 7	255.500	165 ± 13	0.001 ± 0.000	248 ± 24	0.002 ± 0.001	273 ± 55	0.002 ± 0.001
MIL 090073,6		143 ± 6	0.003 ± 0.001	222 ± 8	0.005 ± 0.001	283 ± 14	0.005 ± 0.001
MIL 090152,6	40.360	146 ± 11	0.042 ± 0.016	248 ± 4	0.160 ± 0.023	318 ± 4	0.126 ± 0.011
MIL 090152,7		157 ± 10	0.069 ± 0.011	242 ± 3	0.159 ± 0.018	322 ± 20	0.123 ± 0.014
MIL 090227,6	62.810	128 ± 3	0.032 ± 0.005	202 ± 3	0.062 ± 0.010	300 ± 5	0.041 ± 0.007
MIL 090227,7		129 ± 2	0.035 ± 0.003	207 ± 3	0.059 ± 0.008	279 ± 2	0.034 ± 0.003
MIL 090293,6	7.080	129 ± 4	0.054 ± 0.007	201 ± 3	0.143 ± 0.021	271 ± 7	0.100 ± 0.017
MIL 090293,7		129 ± 5	0.062 ± 0.005	194 ± 4	0.139 ± 0.011	270 ± 10	0.095 ± 0.012
MIL 090480,6	65.418	135 ± 5	0.115 ± 0.023	212 ± 15	0.282 ± 0.023	287 ± 19	0.205 ± 0.021
MIL 090480,7		162 ± 30	0.037 ± 0.004	255 ± 23	0.058 ± 0.015	357 ± 10	0.052 ± 0.010
MIL 090543,3	4.790	125 ± 13	0.058 ± 0.006	215 ± 13	0.157 ± 0.035	317 ± 7	0.103 ± 0.022
MIL 090543,4		109 ± 11	0.057 ± 0.012	202 ± 25	0.101 ± 0.008	304 ± 14	0.069 ± 0.008
MIL 090705,4	4.860	120 ± 10	0.036 ± 0.005	186 ± 2	0.087 ± 0.012	249 ± 3	0.063 ± 0.009
MIL 090705,5		125 ± 2	0.007 ± 0.002	195 ± 2	0.012 ± 0.002	280 ± 22	0.007 ± 0.004
MIL 090785,8	90.340	135 ± 1	0.032 ± 0.003	219 ± 3	–	306 ± 9	–
MIL 090785,9		143 ± 2	0.039 ± 0.005	222 ± 5	–	308 ± 9	–
MIL 090821,5	1.300	126 ± 9	–	186 ± 2	–	239 ± 31	–
MIL 090821,6		130 ± 5	0.019 ± 0.002	195 ± 2	0.033 ± 0.004	270 ± 205	0.020 ± 0.004
MIL 090890,5	5.530	117 ± 12	0.049 ± 0.003	191 ± 7	0.116 ± 0.016	256 ± 5	0.061 ± 0.008
MIL 090890,6		127 ± 8	0.046 ± 0.007	197 ± 5	0.089 ± 0.008	261 ± 3	0.056 ± 0.007
MIL 090891,5	6.950	152 ± 10	0.030 ± 0.001	225 ± 23	0.037 ± 0.002	281 ± 10	0.031 ± 0.001
MIL 090891,6		127 ± 5	0.024 ± 0.002	188 ± 10	0.024 ± 0.003	257 ± 11	0.018 ± 0.003
MIL 090897,3	2.510	125 ± 13	0.039 ± 0.004	217 ± 4	0.134 ± 0.052	316 ± 8	0.098 ± 0.036
MIL 090897,4		–	–	185 ± 3	0.158 ± 0.009	288 ± 29	0.119 ± 0.007
MIL 090907,3	1.780	–	–	209 ± 2	0.164 ± 0.012	335 ± 25	0.117 ± 0.013
MIL 090907,4		–	–	206 ± 11	0.078 ± 0.010	323 ± 9	0.050 ± 0.006
MIL 090915,4	7.342	–	–	198 ± 4	0.148 ± 0.017	290 ± 10	0.112 ± 0.016
MIL 090915,5		–	–	212 ± 18	0.285 ± 0.031	309 ± 19	0.237 ± 0.031
MIL 090919,4	3.865	–	–	223 ± 35	0.173 ± 0.006	328 ± 5	0.160 ± 0.005
MIL 090919,5		–	–	196 ± 7	0.174 ± 0.058	323 ± 20	0.147 ± 0.054
MIL 090967,5	0.310	115 ± 5	0.066 ± 0.003	191 ± 7	0.156 ± 0.022	256 ± 5	0.082 ± 0.010
MIL 090967,6		127 ± 8	0.046 ± 0.007	197 ± 5	0.089 ± 0.008	261 ± 3	0.056 ± 0.007
MIL 090983,4	1.460	169 ± 17	0.002 ± 0.001	–	–	300 ± 30	0.002 ± 0.001
MIL 090983,5		140 ± 11	0.008 ± 0.001	216 ± 9	0.003 ± 0.001	–	–
MIL 090988,4	3.840	120 ± 6	0.100 ± 0.028	185 ± 18	0.202 ± 0.065	259 ± 12	0.120 ± 0.054
MIL 090988,5		143 ± 2	0.054 ± 0.004	220 ± 4	0.101 ± 0.047	287 ± 1	0.085 ± 0.018
MIL 090989,4	2.090	147 ± 5	0.051 ± 0.027	222 ± 10	0.095 ± 0.062	302 ± 30	0.082 ± 0.008
MIL 090989,5		132 ± 19	0.027 ± 0.002	223 ± 20	0.028 ± 0.001	282 ± 21	0.024 ± 0.001
500 mg samples							
MIL07182,11	111.98	132 ± 3	0.009 ± 0.003	205 ± 5	0.020 ± 0.006	278 ± 3	0.016 ± 0.005
MIL07182,12		115 ± 5	0.049 ± 0.010	195 ± 5	0.104 ± 0.016	289 ± 12	0.075 ± 0.010
MIL090019,9	793.80	120 ± 5	0.021 ± 0.003	200 ± 9	0.043 ± 0.002	291 ± 10	0.028 ± 0.001
MIL090019,10		135 ± 5	0.027 ± 0.001	213 ± 6	0.053 ± 0.017	310 ± 10	0.030 ± 0.012

* Masses quoted are the original mass of the parent meteorite, taken from the Antarctic Meteorite database (http://curator.jsc.nasa.gov/antmet/us_clctn.cfm) in October 2014. The significant figures quoted are as given in the database. Uncertainties on the TL data are one sigma based on triplicate measurements.

Table 4
Induced thermoluminescence data for Dominion Range (DOM) samples.*

Meteorite	Parent	Peak 1		Peak 2		Peak 3	
	Mass (g)	Peak T (°C)	TL sensitivity (Dhajala = 1)	Peak T (°C)	TL sensitivity (Dhajala = 1)	Peak T (°C)	TL sensitivity (Dhajala = 1)
50 mg samples							
DOM 08139,6	19.460	150 ± 15	0.0850.011	230 ± 23	0.207 ± 0.026	313 ± 3	0.183 ± 0.030
DOM 08139,7		150 ± 15	0.169 ± 0.019			278 ± 6	0.716 ± 0.047
DOM 10104,8	192.289	150 ± 16	0.102 ± 0.016	237 ± 12	0.028 ± 0.003	320 ± 32	0.330 ± 0.033
DOM 10104,9		153 ± 6	0.294 ± 0.038	235 ± 23	0.490 ± 0.075	350 ± 10	0.394 ± 0.064
DOM 10121,6	14.983	152 ± 4	0.104 ± 0.009	267 ± 13	0.181 ± 0.053	373 ± 3	0.286 ± 0.085
DOM 10121,7†							
DOM 10299,6	13.834	141 ± 10	0.036 ± 0.003	242 ± 14	0.080 ± 0.005	336 ± 12	0.078 ± 0.003
DOM 10299,7		129 ± 8	0.020 ± 0.005	211 ± 20	0.041 ± 0.004	309 ± 19	0.031 ± 0.005
DOM 10900,5	22.707	117 ± 7	0.008 ± 0.004	196 ± 7	0.014 ± 0.005	300 ± 25	0.009 ± 0.004
DOM 10900,6		125 ± 13	0.009 ± 0.002	207 ± 5	0.013 ± 0.000		
500 mg samples							
DOM10104,18	192.289	140 ± 3	0.057 ± 0.013	206 ± 4	0.120 ± 0.013	278 ± 3	0.107 ± 0.013
DOM10104,19		150 ± 5	0.041 ± 0.018	225 ± 5	0.071 ± 0.025	295 ± 5	0.071 ± 0.016
DOM10900,9	22.707	123 ± 18	0.0013 ± 0.0002	202 ± 10	0.0025 ± 0.0008	nd	nd
DOM10900,10		128 ± 10	0.0015 ± 0.0003	198 ± 3	0.0028 ± 0.0006	290 ± 14	0.0012 ± 0.0001

* Masses quoted are the original mass of the parent meteorite, taken from the Antarctic Meteorite database (http://curator.jsc.nasa.gov/antmet/us_clctn.cfm) in October 2014. The significant figures quoted are as given in the database. Uncertainties on the TL data are one sigma based on triplicate measurements.

† Data are not reported for this chip since the sample was dominated by an EGG4-like CAI.

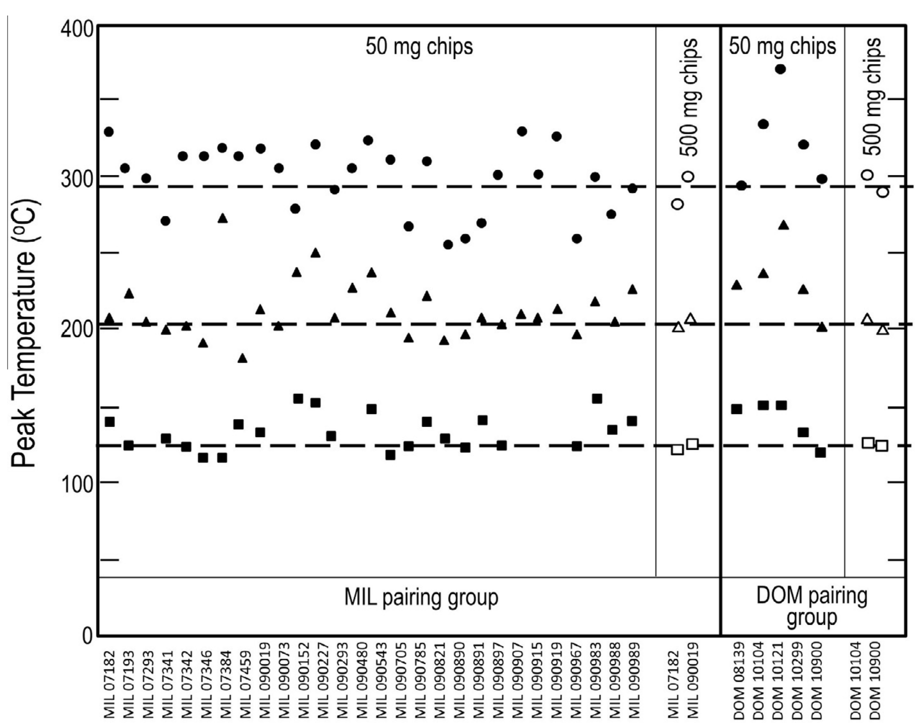

Fig. 3. A comparison of the positions of resolvable peaks (including strong inflections) in the glow curves of the present CO chondrites. Three discernable peaks are present, at ~120 °C, ~200 °C, and ~300 °C which is in agreement with earlier studies of CO chondrites (Keck and Sears, 1987; Sears et al., 1991). These three peaks have been ascribed to low-feldspar, high-feldspar, and refractory minerals respectively (Guimon et al., 1995). While the 50 mg chips show more scatter in the data, especially for the Dominion Range meteorites, they are in agreement with the data for the 500 mg samples.

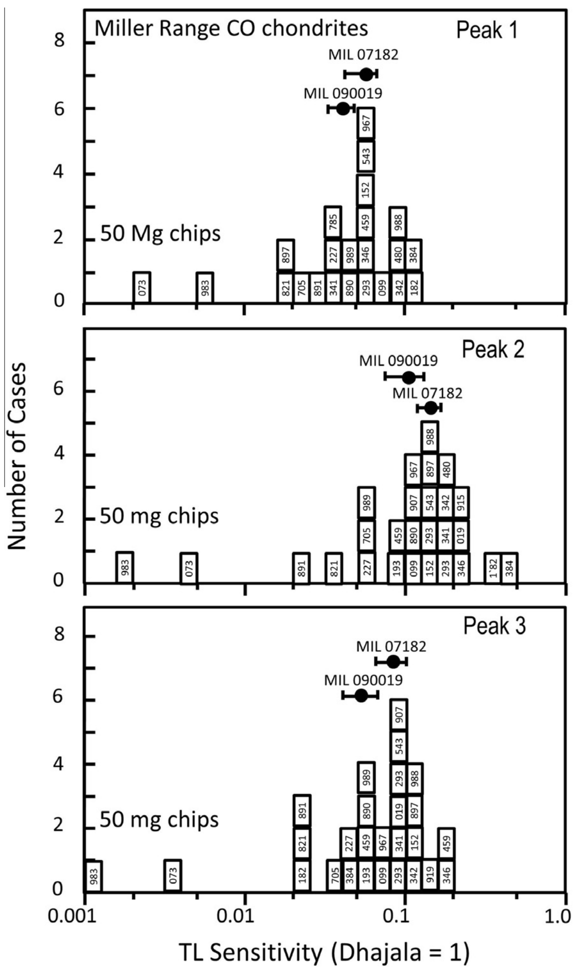

Fig. 4. Histograms for the TL sensitivity for 50 mg chips of the present Miller Range CO chondrites for peak 1 (∼120 °C), peak 2 (∼200 °C), and peak 3 (∼300 °C). Reasonable strong histograms are observed with for peak 1and peak 3 (∼0.05) and peak 2 (∼0.2). Also shown are the data for the 500 mg chips which show the same relative trend but seem displaced downwards by a factor of about two.

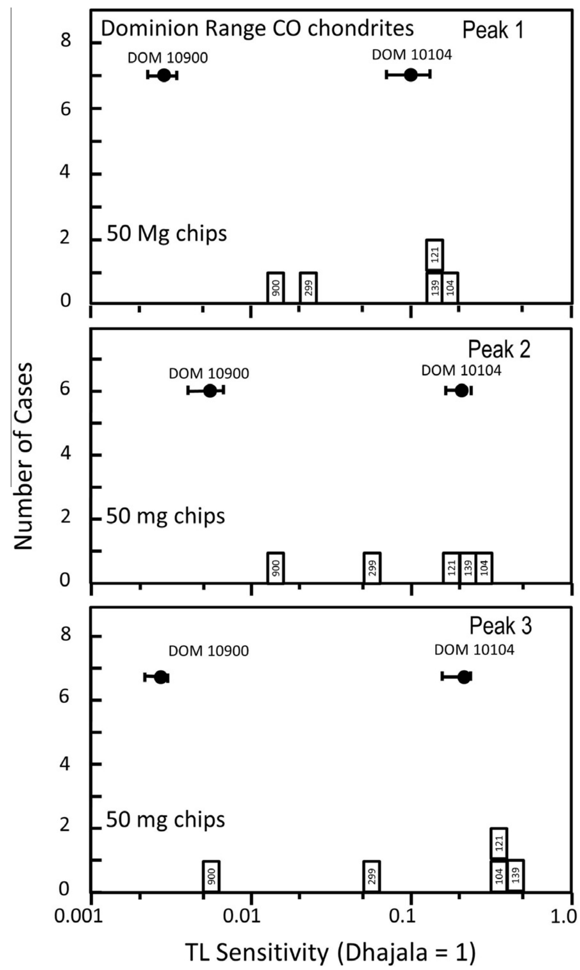

Fig. 5. Histograms of the mean TL sensitivities of two 50 mg chips of the Dominion Range CO chondrites studied here for peak 1 (∼120 °C), peak 2 (∼200 °C), and peak 3 (∼300 °C). Also shown are the values the means of two 500 mg chips of MIL 07182 and MIL 090019 which also show a large spread. The values for the larger chips are about a factor of two lower than the peaks of the histograms because of the influence of the low TL samples on these non-linear distributions.

quantitative information from small samples of heterogeneous meteorites. I will discuss the implications of the present data by first looking at pairing and heterogeneity, then natural TL orbits and terrestrial age, and then the induced TL and petrographic type. Finally, I present some notes on the objectives and methods for the classification of meteorites by metamorphic alteration.

4.1. Pairing of the Dominion Range and Miller Range CO chondrites

The clustering of the natural TL data shown in Fig. 2 is consistent with most of the MIL samples being paired; however the peaks in the histogram are fairly broad. Some variation in the natural TL of a given meteorite is to be expected because of shielding and dose rate variations through the stone. These are much less than commonly observed for cosmogenic isotopes because ionization is a much lower energy process than spallation. Measurements of cosmogenic natural TL profiles were reviewed by Sears et al. (2013). In a large slab of the Estacado meteorite, about 55 cm by 40 cm, natural TL covered a range of about 10% although smaller meteorites seem to have steeper profiles. Benoit and Sears (1994) reported theoretical calculations that showed that a 20 cm meteorite would have a profile with a 5% range in its natural TL while for 50 cm this would be 15%. Thus the clusters and the spread observed in Fig. 2 are consistent with all the MIL meteorites being paired.

The position of the induced TL peaks in the present meteorites (Fig. 3) are governed by mineralogy and is similar for all the CO chondrites reported here and in earlier and thus has no bearing on pairing studies (Keck and Sears, 1987; Sears et al., 1991). However, TL sensitivity varies over three orders of magnitude within the CO chondrite class and does have value as a discriminator for pairing. In the case of the 50 mg chips of MIL CO chondrites, there is essentially a single log-normal distribution suggesting a single population with a value is in agreement with the data for the 500 mg chips (Fig. 4). There are two outliers, MIL 090983 and MIL 090073, which also have anomalously low natural TL. For MIL 090983 I can ascribe to this sample being taken too close to the fusion crust. The masses of the original meteorite was 1.46 g.

While I measured the TL sensitivity of 29 MIL CO chondrites, 204 CO chondrites have been found at the Miller Range and it seems likely they are all paired. In Fig. 6 the mass distributions of the present MIL CO chondrites are compared with that of all the CO chondrites recovered from this location. Given the relatively small number in the present study, it does seem that they have the same mass distribution as all MIL CO chondrites which suggest that the present sample is representative and that all MIL CO chondrites are paired.

The situation with the DOM CO chondrites is different and difficult to interpret because I have relatively few samples. It seems reasonable to argue that the coincidence in find location and the common class and type are strong evidence that all the DOM CO chondrites are paired. The spread in TL sensitivity might then be attributed to a brecciated and heterogeneous parent meteorite. I am not sure this conclusion is correct. As mentioned previously and discussed in the next section, the variations in natural TL suggest that some samples may have a different orbit and terrestrial age history to the others. The low natural TL values cannot be ascribed to sampling too close to the fusion crust because all the samples are quite large, the original parent masses were all >14 g. It seems most likely, as incredible as it seems, that there are two or three discrete falls of CO chondrites among the CO chondrites collected at Dominion Range.

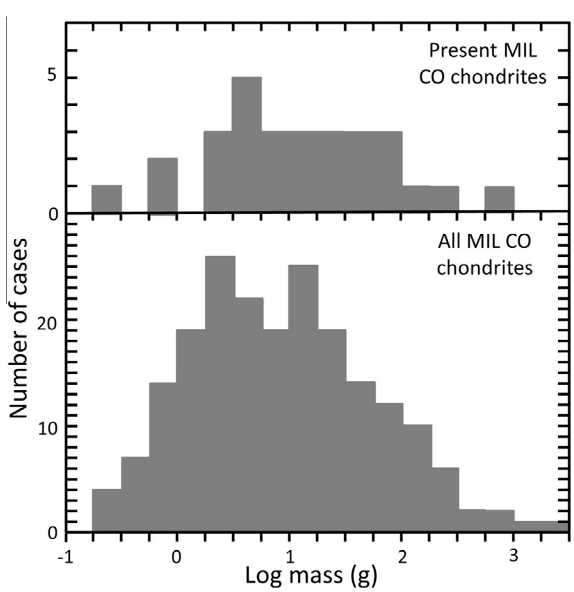

Fig. 6. Histograms of the parent masses of the present MIL CO chondrites with all 203 CO chondrites recovered to date from the Miller Range. Notwithstanding the small number of samples in the present study, it seems that the mass distributions are similar for the two populations and that the present samples are representative and therefore that all the Miller Range CO chondrites are paired.

4.2. Heterogeneity and brecciation of the Dominion Range and Miller Range CO chondrites

The MIL CO chondrites are remarkably uniform in natural TL. Not only do the components of the meteorite share a common thermal and radiation history, the method allows for mineralogical and petrographic variations through an internal normalization. As would be expected for meteorites as low in petrologic type as MIL the TL sensitivity shows greater spread, but clearly there is a preferred value. The statement made 35 years ago that the petrologic type assigned on the basis of TL sensitivity could be uncertain by plus or minus one petrologic type picked up on this possible spread although the situation has not been rigorously quantified before this study. There is no evidence in these data for brecciation in MIL.

As discussed in the previous section, the data for DOM CO chondrites appear to be extremely heterogeneous, but it seems likely that this is due to the presence of more than one meteorite rather than them being a paired heterogeneous and brecciated meteorite. This is not withstanding the small number of DOM meteorites I have in this study.

4.3. Orbit and terrestrial ages of MIL and DOM

The level of natural TL of a meteorite is determined by equilibrium between the rate of build-up and the rate of decay and may be described by the equation:

$$\phi = \phi_s/\{1 + [s/\alpha R \exp(-E/kT)]\} \quad (1)$$

where ϕ is the level of natural TL, ϕ_s is the value of TL at saturation, R is the radiation dose rate, and α is a rate constant, E is the activation barrier for TL decay, T is temperature (K), k is Boltzmann's constant, and s the Arrhenius constant (Sears et al., 2013). The Arrhenius constant is sometimes known as the pre-exponential factor or the "attempt-to-escape" constant and it captures the likelihood of an electron having sufficient energy to overcome the activation barrier, E. Typical values for E are 1–2 eV and typical values for s are 10^{10}–10^{12} s^{-1} (McKeever, 1980). Thus there are two environmental terms, R and T, the remainder being determined by the solid state properties of the mineral producing the TL signal (normally feldspar). The important temperature is that at perihelion and it can be calculated from:

$$T = 279(\theta/d^2)^{1/4} \quad (2)$$

where θ = the ratio of the absorbed radiation to that of the emitted radiation and d is the perihelion distance. Hence natural TL levels for a meteorite when it enters the atmosphere depend, in large part, on perihelion (Melcher, 1981a; Benoit et al., 1991).

With the increasing number of meteorites with film and video data for their fall, now at 20, precise orbits are known and a comparison of their natural TL values would be most interesting. I am currently measuring the natural TL properties of observed falls with published orbits and to date the Saricicek howardite has a natural TL orbit estimate is very close to the perihelion reported by analysis of its trajectory.

Once on Earth the natural TL decays at a rate given by (to a reasonable approximation):

$$d\phi/dt = -s\phi_o \exp(-E/kT) \quad (3)$$

where t is time (terrestrial age). Eq. (3) is the basis of terrestrial age determination using natural TL (Melcher, 1981b; Benoit et al., 1993).

Fig. 7 is a plot taken from Benoit et al. (1993) comparing the predictions of these relationships with the observed data for Antarctic meteorites. In this case, the terrestrial ages were determined by ^{36}Cl measurements (Nishiizumi et al., 1979). Most Antarctic meteorites (indicated by filled squares in Fig. 7) plot between theoretical lines predicted by decay at temperatures between 0 °C and −5 °C. A few (indicated by open squares), usually around 5% of the data set, plot at much lower natural TL levels than can be explained by these theoretical lines. These 5% are noted not just for their low natural TL, but also for high ^{26}Al activity. They are commonly attributed to meteorites that were on orbits with small perihelia and high radiation environment. They have lower natural TL because of thermal draining but lower temperature traps are populated suggesting recent radiation exposure (Hasan et al., 1987; Sears et al., 2011). Since they are low temperature TL traps (i.e. they have relatively low values of E), they fade quickly, dropping two orders of magnitude in about 150 ka.

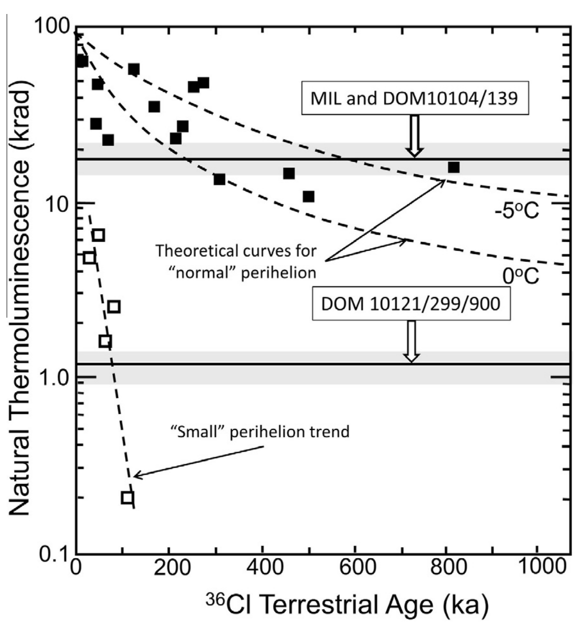

Fig. 7. The natural TL of Antarctic meteorites compared with the terrestrial age as determined by ^{36}Cl abundance (figure from Benoit et al., 1993). The filled squares are meteorites with normal perihelion (say 0.8–1 AU), and the open squares are meteorites with small perihelion (>0.8 AU, usually ~0.6 AU) whose TL decays rapidly. (See Sears et al., 2011, for a discussion.) Superimposed on this plot are the means (with ±1σ shown as the shaded regions) for (1) upper line, the MIL meteorites and DOM 08139/10104 which have natural TL consistent with membership of the "normal" perihelion group and terrestrial ages ~600 ka, and (2) DOM 10121/10900 which have natural TL values too low to be explained alone by a large terrestrial age and which must have had small perihelion and terrestrial age of ~100 ka.

Superimposed on Fig. 7 are two horizontal lines indicating the natural TL values of the present meteorites, with shading indicating ±1σ. The MIL CO3 chondrites and DOM 08139/10104 plot on the trend line suggesting terrestrial ages of ~300–600 ka, while the DOM 10121/10299/10900 meteorites plot on a line giving them a terrestrial ages of ~100 ka. The perihelia for DOM 10121/10900 are probably 0.7–0.8 AU, compared with the "normal" value of 0.9–1.0 AU Benoit and Sears (1994). The dependence of natural TL on perihelion and how it is affected by differences in radiation dose was shown in Fig. 3b of Benoit et al. (1991). A natural TL of 10 krad, for example, corresponds to a perihelion for a dose rate of 10, 1, and 0.1 rad/year of 0.8, 0.9, and 1.0 AU, respectively. Thus dose rate variations of 10–20% as discussed above will not significantly affect the predicted perihelion. Variations due to factors other than dose rate are more difficult to quantify, the most important is probably the complexity of the glow curve and variations in E and s, so that a rigorous application of luminescence theory to observed data really calls for a complete modeling of the glow curve. In the meantime, these differences in inferred perihelia should be regarded as semi-quantitative.

For many years it seemed that it was easy to distinguish low natural TL due to long terrestrial ages from low natural TL due to small perihelion. With increasing terrestrial age natural TL tends to trend asymptotically to 5 krad. However, in every data base assembled, ordinary chondrites, basaltic meteorites, meteorites from various Antarctic fields, lunar meteorites, and others, about 20% of the samples had natural TL below 5 krad, sometimes considerably lower (Fig. 5). It was concluded that in all groups, about 20% had small perihelia (Sears et al., 2013). However, in a study of the natural TL of 120 chondrites for which ^{26}Al data were available, an intermediate group was identified in which there was ambiguity (Sears et al., 2011). Thus a value of 5–10 krad, maybe as high as ~15 krad, does carry some ambiguity and could be due to a normal perihelion and large terrestrial age or a small perihelion and a short terrestrial age.

4.4. Metamorphic history of the DOM and MIL CO chondrites

4.4.1. *Thermoluminescence and Mineralogy of CO chondrites*

The broad hummocky peaks displayed by the CO chondrites in the present study are characteristic of low petrographic type meteorites, whether type 3 ordinary chondrites, CO chondrites, or CV chondrites (Sears et al., 1980; Keck and Sears, 1987; Guimon et al., 1995). The peak temperatures observed are also similar to previous studies of CO chondrites, and are fairly characteristic of CO chondrites (Sears et al., 1991). Detailed TL and cathodoluminescence studies have shown that the peak at ~120 °C is due to feldspar in the low-temperature (ordered) form and the peak at ~210 °C is due to feldspar in the high-temperature form. The peak at ~350 °C is due to refractory minerals like gehlenite, or akermanite (Guimon et al., 1995).

In addition to a large number of studies on meteorites, recently reviewed by Sears et al. (2013), there are TL studies of terrestrial feldspars (Benoit et al., 2001) and cathodoluminescence studies of meteorites and lunar samples (Akridge et al., 2004) that confirm and enhance the conclusions drawn from meteorites. The formation of crystalline feldspar from a feldspathic glass during metamorphism is the major process driving the 10^5-fold increase in TL sensitivity observed for ordinary chondrites, and the effect is enhanced slightly by a spectral shift that accompanies the homogenization of feldspar compositions.

4.4.2. *Thermoluminescence sensitivity as measure of metamorphic alteration*

Thermoluminescence has a large dynamic range and high precision and, when first reported, was capable of distinguishing differences in metamorphism in type 3 ordinary chondrites that no other technique could detect (Sears et al., 1980). Olivine composition and heterogeneity for example are very similar over the range of type 3.0 to type 3.4. While the thermoluminescence sensitivity range is 10^5-fold for ordinary chondrites, there is a 10^3-fold range for type 3 ordinary chondrites, and a 100-fold range in CO3 chondrites. TL sensitivity can typically be measured within a factor of two, often much less judging from triplicate measurements. Soon after the publication of the 3.0–3.9 subdivision of type 3 ordinary chondrites, variations in presolar diamond and H isotope ratios were discovered that correlated with TL sensitivity (Huss et al., 1981; McNaughton et al., 1981). Most recently it has been observed that, in addition to low types containing Ca in their olivine (Dodd et al., 1967; Scott and Taylor, 1983), the olivine in the low petrologic also types contains Cr (Grossman and Brearley, 2005).

Grossman and Brearley (2005) looked for correlations between the TL sensitivity of 3.0–3.2 chondrites and Cr in the olivine (they could also have used Ca in the olivine; Dodd, 1972) and did not find such a correlation. First, the accuracy of the TL measurement is confirmed by other data sets as mentioned above, such as H isotopes, pre-solar diamonds, and, most significantly, cathodoluminescence images. On the other hand, the Grossman and Brearley rankings were based on a highly subjective ordering of histograms which could be viewed other ways. I see no justification for subdivision beyond the 0.1 increments based on existing data.

Induced TL measurements provide an indication, not just of the general level of metamorphic alteration, but of the time–temperature curve for meteorite metamorphism. It is worth stressing that while the intensity of the TL signal reflects the overall level of alteration, the temperature and width of the TL signal provides an indication of postmetamorphic cooling. While not yet quantitative, although this possibility certainly exists, this has been demonstrated by comparing the TL data with cooling rates calculated from Ni profiles in kamacite and taenite (Benoit and Sears, 1993). Recognizing the existence of different temperature–time histories, as with distinguishing between peak metamorphic temperatures and closure temperatures, are essential in understanding the history of the meteorites and, while such a history affects other types of data, it may not be immediately obvious in those cases.

4.4.3. *Principal component analysis and correlations among the quantitative petrologic type parameters*

In view of the relatively large amount of quantitative data available on the CO chondrites that appears to reflect metamorphic alteration, a Principal Components Analysis was performed using the Varimax method of rotation and the Kaiser normalization. The software used was the SPSS marketed by IBM. The analysis extracted three components that explained 83% of the variance in the data set. Component 1 contained parameters relating to bulk composition, bulk carbon, the inert gases, and the reflectivity at 0.8 μm, which presumably reflects bulk carbon, and it explained 30% of the variance. Component 2 contained parameters that underwent transformations in response to metamorphism that did not involve significant bulk diffusion, essentially TL sensitivity and matrix composition, with a minor contribution from carbon ordering, and it explained 28% of the variance in the data. The third component involved the diffusion of iron throughout the meteorite and was dominated by mol Fa and Ni in the metal and it accounted for 25% of the variance.

These results indicate, that for the CO chondrites at least, no one parameter stands out as overwhelmingly valuable in assessing the level of metamorphism experienced. This comes as no surprise considering the complexity of the meteorites and the experimental uncertainties associated with all these techniques. However, since TL sensitivity is clearly one of the more robust techniques for assessing metamorphic alteration in chondrites and most widely applied, and needing some point of comparison, TL sensitivity is next compared with the other available measurements. A series of log TL sensitivity vs. parameter plots are shown in Fig. 8. The TL data for these plots were taken from Keck and Sears (1987) and Sears et al. (1991), the mineralogical data come from a variety of source cited below.

4.4.3.1. TL sensitivity vs. olivine composition. A plot of log (TL sensitivity) against olivine composition is shown in Fig. 8a, using the sources for olivine data given by Sears et al. (1991). Olivine compositions for CO chondrites range from about 10 to 25 mol% Fa, a factor of 2.5. The correlation has an R^2 of 0.64 ($n = 17$) but it is necessary to include finds to see a correlation. In fact, Fig. 8a includes several anomalous C chondrites that plot at the lower end of the trend. See Sears et al. (1991) for a discussion.

4.4.3.2. TL sensitivity vs. olivine heterogeneity. Olivine heterogeneity is compared with TL sensitivity in Fig. 8b; again the sources of data are given by Sears et al. (1991). Without the falls, there is a two point correlations (Warrenton and the rest) but including the finds (which show considerable scatter) the correlation has an R^2 of 0.56 ($n = 14$).

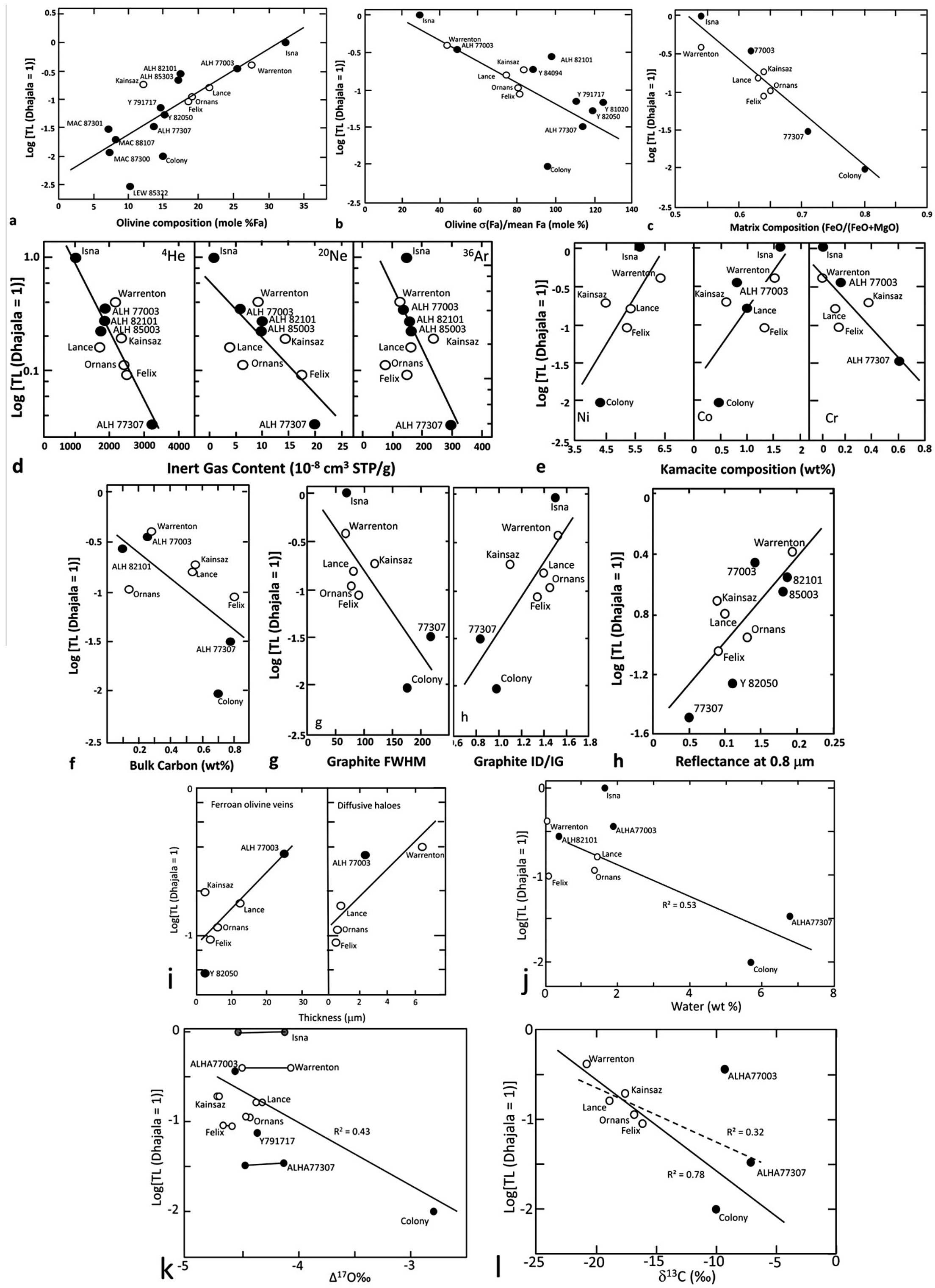

Fig. 8. The log of the TL sensitivity of CO chondrites (y-axis) compared with several properties that are sensitive to parent metamorphism (x-axis). The trends lines are regression lines, R^2 values are given in the text. (a) Olivine composition, mol% (Sears et al., 1991, and references therein); (b) olivine heterogeneity, olivine σ(Fa)/mean Fa, mol%, (Sears et al., 1991, and references therein); (c) matrix composition, FeO/(FeO + MgO), (Scott and Jones, 1990); (d) inert gas content, 10^{-8} cm^3 STP/g, ^{4}He, ^{21}Ne, ^{36}Ar (Schultz and Franke, 2004; Bartoschewitz et al., 2010); (e) kamacite composition, wt%, Ni, Co, Cr (McSween, 1977); (f) bulk carbon, wt% (Wiik, 1969; Jarosewich, 1990; Greenwood and Franchi, 2004); (g) ordering of the graphite, graphite FWHM, graphite ID/IG (Bonal et al., 2007); (h) reflectance at 0.8 mm (Cloutis et al., 2012); (i) behavior of the AOI, i.e. thickness of ferroan olivine veins, and thickness of diffusive haloes, µm (Chizmadia et al., 2002); (j) concentration of water, wt% (Wiik, 1969; Jarosewich, 1990); (k) oxygen isotopes in terms of Δ^{17}O, ‰, (Clayton and Mayeda, 1999; Greenwood and Franchi, 2004, instances of disagreement are indicated with tie-lines); (l) carbon isotopes (δ^{13}C, ‰) from Greenwood and Franchi, 2004).

4.4.3.3. TL sensitivity vs. matrix composition. The TL sensitivity data are compared with the matrix compositions from Scott and Jones (1990) in Fig. 8c. Matrix FeO/(FeO + MgO) values range from 0.54 to 0.80, a range of a factor of 1.5. There is an excellent correlation with $r^2 = 0.92$ ($n = 9$). There is no difference between falls and finds, although the matrix might be expected to be highly prone to contamination. In fact, it is really the finds that define the line since the falls are clustering in the middle of the trend. Somewhat surprisingly, there is no indication in this figure that the data for finds have been influenced by weathering.

4.4.3.4. TL sensitivity vs. inert gas content. Fig. 8d shows plots of log (TL sensitivity) against trapped inert gases from the compilation of Schultz and Franke (2004). ^{4}He, ^{21}Ne, and ^{36}Ar show ranges of 917–2433, 0.86–20.1, 58.7–14.75·10^{-8} cm^3 STP/g, factors of 2.7, 23, and 2.4, respectively. Helium-4 shows an insignificant correlation ($R^2 = 0.30$) but this rises to $R^2 = 0.78$ ($n = 10$) with the exclusion of Colony. The same is true of ^{21}Ne, not significant with Colony ($R^2 = 0.26$) but significant without ($R^2 = 0.58$, $n = 10$). The justification for removing Colony is its severe weathering; meteorites from the Prairie States show a particularly severe and resilient weathering. Argon-36 is not significant with or without Colony ($R = 0.0$ with and 0.23 without). Bartoschewitz et al. (2010) argued for the absence of trends between inert gas content and petrologic type, but their study included only the six falls and, as we have seen here, many of these trends are only apparent when the finds are included because so many of the finds are of low petrologic type.

4.4.3.5. TL sensitivity vs. metal composition. The Ni, Co, and Cr content of the kamacite are shown in Fig. 8e, data from McSween (1977). The Ni content of the kamacite ranges from 4.7 to 6.3 wt%, while Co and Cr range from 0.35 to 1.6 and <0.1 to 0.56 wt%, respectively. Thus the ranges are by factors of 1.3, 4.6, and >56, for Ni, Co, and Cr respectively. The data are few but all show weak correlations ($R^2_{Ni} = 0.52$, $R^2_{Co} = 0.46$, $R^2_{Cr} = 0.63$) and all these trends are dependent on finds, the falls again clustering in the middle of the diagram.

4.4.3.6. TL sensitivity vs. bulk carbon content. There is a weak correlation between log (TL sensitivity) and bulk carbon (Fig. 8f), ($R^2 = 0.44$, $n = 9$). The range in carbon abundance is 0.1–0.8 wt%, a factor of 1.8. Carbon data have been taken from the compilation of Greenwood and Franchi (2004) with the addition of data from Wiik (1969) and Jarosewich (1990). The trend among the falls would be strong without Ornans, but falls and finds seem to be equally responsible for the observed correlation.

4.4.3.7. TL sensitivity vs. graphite ordering. The width of the D band in the Raman spectrum for organics in the CO chondrites in the Bonal et al. (2007) study ranges from 60 to 211 cm^{-1}, a factor of 3.5 range, with uncertainties from 3% to 13%. The tiny dynamic range and comparatively large uncertainties make ordering of the carbon one of the less useful paleothermometry techniques. Nevertheless, there is a reasonable correlation with TL sensitivity, $R^2 = 0.62$ ($n = 8$) but again the falls cluster in the middle of the range and the trend is dependent on the finds (Fig. 8g). This is troublesome since, as is well-known and recently emphasized by Greenwood and Franchi (2004), carbon is prone to contamination. Other problems with the technique are common to all geothermometers. For example, there is no way to determine with absolute certainty the factors determining closure of the system.

Bonal et al. have argued that this technique can be applied across the classes, but this is unlikely because: (1) the amorphous carbon may have different origins and different starting physical and compositional properties; (2) the environment for each class may different, for instance of trace constituents like alkalis and halogens have a major influence on disordering (Chung et al., 1977), water may vary, side reactions that remove impurities may differ, especially if they are redox reactions which will differ from class to class; (3) the physical history of the classes may vary, for example the radiation environment will influence graphite ordering. The vast literature in the coal and oil industry testifies to the complexity of the organic geochemistry of graphitization (e.g. Engel and Macho, 1993).

The band ratio for the organics in CO chondrites ranges from 0.83 to 1.50, a factor of 1.8, with uncertainties ranging from 2% to 9% (Bonal et al., 2007). As with peak width, there is a reasonable correlation, $R^2 = 0.59$ ($n = 8$) but again the trend is dependent on finds (Fig. 8g).

4.4.3.8. TL sensitivity vs. reflectivity at 0.8 μm. The spectral reflectivity of ten CO chondrites for which TL data exist were reported by Cloutis et al. (2012). The data in Fig. 8h were read from their Fig. 5. The reflectivity of these meteorites at 0.8 μm ranged from 0.05 to 1.95, a factor of 39, with uncertainties probably in the order of 5% (judging from the noise on the spectra). As pointed out by Cloutis et al., the correlation between log TL sensitivity and reflectance is quite reasonable, $R^2 = 0.60$ ($n = 10$).

4.4.3.9. TL sensitivity vs. properties of refractory inclusions. Russell et al. (1998) described, in some detail, the changes occurring to the Ca–Al-rich inclusions in CO chondrites with parent body metamorphism. As petrographic type increases, spinel in melilite-rich and coarse-grained spinel-pyroxene inclusions becomes more Fe rich with the development of relatively homogeneous hercynitic spinel, reaching 50–60 mol% by type 3.4. Perovskite converts to ilmenite in type 3.4. Melilite-rich inclusions are abundant in CO3.0–3.3 meteorites, rare in 3.4 meteorites, and absent meteorites of types 3.5–3.7 (replaced by inclusions rich in feldspathoids, pyroxene, and Fe-rich spinel). Furthermore, disturbance of the magnesium–aluminum systematics may be more severe in higher petrologic types.

For the ameboid olivine inclusions, Chizmadia et al. (2002) reported their data in a more quantitative form; namely, in terms of the ferroan olivine vein thickness and the thickness of diffusive haloes around the AOI (Table 5). The thickness of the veins and the haloes ranges over a factor of about 10. Fig. 7i shows the data in graphical form,

Table 5
The AOI characteristics use to refine the CO3 petrographic subtypes (Chizmadia et al., 2002)[*].

Petrographic type	Thickness of ferroan olivine veins (μm)	Thicknesses of diffusive haloes (μm)
3.0	n/a	n/a
3.1	<2	n/a
3.2	~2.5	n/a
3.3	~4	~0.5
3.4	~6	~0.6
3.5	10–15	~0.8
3.6	20–30	2–3
3.7	n/a	5–8
3.8	n/a	n/a

[*] n/a means "not applicable".

leaving out the meteorites for which these parameters do not apply (veins; Y 81020, ALH 77307, Colony, Isna: haloes for both parameters; Warrenton for veins, Kainsaz, Y 82050 for haloes. Y 81020, ALH 77307, Colony, Warrenton, Isna). Despite the limitations of few samples and many meteorites being excluded from this parameter, and that the relationship appears to be more log–log than log-linear, there is actually a good log-linear correlation with TL sensitivity and thickness of the veins ($R^2 = 0.61$, $n = 6$) and haloes ($R^2 = 0.71$, $n = 5$).

4.4.3.10. TL sensitivity vs. water concentration. Wiik (1969) and Jarosewich (1990) have measured the water content of nine CO chondrites and the concentrations vary by nearly a factor of 20. The data show a weak correlation with TL sensitivity ($R^2 = 0.52$, $n = 9$), where ALHA77307 and Colony have high water and low TL sensitivity while the remainder cluster weakly with low water and relatively high TL sensitivity (Fig. 8j).

4.4.3.11. TL sensitivity vs. isotopic properties (O, and C). The data for oxygen isotopes are shown in Fig. 8k. The data from Clayton and Mayeda (1999) and Greenwood and Franchi (2004) do not always agree well and their data for the same meteorite are linked with tie lines in the figure. The R^2 value is 0.43 ($n = 10$), but again the correlation depends on Colony with especially low TL sensitivity and relatively small $\Delta^{17}O$. The remaining data show a relatively small range of $\Delta^{17}O$ but a large spread of TL sensitivity values.

Carbon isotopes (Greenwood and Franchi, 2004) also show a correlation with TL sensitivity ($R^2 = 0.32$, $n = 8$), see Fig. 8l. ALHA77003 has a surprisingly low $\delta^{13}C$, probably a weathering effect. Without ALHA77003, the $R^2 = 0.78$ ($n = 7$).

4.4.4. Notes on petrologic types for chondrites

The petrologic types of CO chondrites, in particular, have been the subject of considerable interest and at least on one occasion the flow of discussion has become confused. It has often been said that a good classification scheme can be a great aid to research and a bad scheme can be equally harmful, and meteorite researchers have long grappled with this. Ultimately, the final test is survivability. Van Schmus and Wood's (1967) scheme has lasted 48 years, the Sears et al. (1980) modification of that scheme has lasted 35. Here are some suggestions I would like to make.

4.4.4.1. The scheme must be specific enough to be meaningful, but broad enough to be simple in application and robust to new developments. It is possible to try to say too much in an overly ambitious classification scheme with the result that the scheme is difficult to apply, difficult to remember, results in many bins with few members, and requires constant revision as new meteorites are reported. A classification scheme is not a ranking.

4.4.4.2. The scheme should be descriptive and not interpretative. When Van Schmus and Wood (1967) published their petrographic type 1–6 definitions, they believed they were a metamorphic sequence. Quickly it was realized that this was probably not so, and that there were two series centered on type 3, to the left (going down) was aqueous alteration, to the right (going up) was metamorphism. The interpretations changed, but the definitions were as useful as ever. Good classification schemes describe the meteorites. They do not depend on interpretations.

4.4.4.3. The scheme should not oversimplify and obscure important details. Trying to define a one-size-fits-all scheme, applicable across the different classes of meteorites, ignores the complexities of real rocks and can be highly misleading. An example is the Bonal et al. (2007) revision of the petrologic types for CO chondrites. By trying to fit the CO chondrites into a scheme devised for CV chondrites, five out of eight meteorites classified have petrologic types that are limits, four out of five without the finds. What little value this has in comparing metamorphism in different classes is lost when comparisons are being made within the class, which is usually the case. In any event, arguing that this scheme applies across the classes ignores the many known differences between the classes discussed above.

4.4.4.4. The scheme should take account of all the available information, reliance on any one technique should be avoided, and single observations based on interpretation should be regarded with caution. The chondrite meteorites must be among the most complicated rock systems known to science. Most, if not all, terrestrial rock systems are clearly the result of a single geological (or geobiological) process

Table 6
Updated definitions for the petrographic types of CO chondrites.*

Type	TL sensi-tivity[a]	Olivine[b]		Matrix[c]	Kamacite composition[d] (wt%)			C[e]	^{20}Ne[f]	Graphite ordering[g]		AOI[h]		Reflectance[i]
	(Dhajala = 1)	Mean Fa (mol%)	σFa/Fa (%)	F/(F+M)	Ni	Co	Cr	(wt%)	10^{-8} cc/g	I_D/I_G	FWHM (D)	D_v (μm)	D_h (μm)	0.8 μm (%)
3.0	<0.017	<11.0	>126	>0.77	<4.4	<0.2	>0.5	>0.65	>19	<0.85	>187	n/a	n/a	<4
3.1	0.017–0.030	11.0–13.5	112–126	0.73–0.77	4.4–4.6	0.2–0.4	0.47–0.50	>0.65	>19	0.85–0.95	175–187	<2	n/a	4–6
3.2	0.030–0.054	13.5–16.0	102–112	0.70–0.73	4.6–4.8	0.4–0.6	0.34–0.47	0.55–0.65	16–19	0.95–1.04	150–175	~2.5	n/a	6–9
3.3	0.054–0.10	16.0–18.5	90–102	0.67–0.70	4.8–5.0	0.6–0.8	0.26–0.34	0.45–0.55	13–26	1.04–1.16	135–150	~4	~0.5	9–12
3.4	0.10–0.17	18.5–21.0	78–90	0.63–0.67	5.0–5.2	0.8–1.0	0.18–0.26	0.35–0.45	10–13	1.16–1.24	115–135	~6	~0.6	12–15
3.5	0.17–0.30	21.0–24.0	64–78	0.60–0.63	5.2–5.4	1.0–18	0.10–0.18	0.25–0.35	10–7 1	1.24–1.34	88–115	10–15	~0.8	15–17
3.6	0.30–0.54	24.0–27.5	46–64	0.57–0.60	5.4–5.7	<0.1	<0.15	0.15–0.25	7–4	1.34–1.43	64–88	20–30	2–3	17–20
3.7	0.54–1.00	27.5–31.0	28–46	0.53–0.57	5.7–6.0	<0.1	<0.15	<0.15	<4	1.43–1.55	54–64	n/a	5–8	20–23
3.8	1.0–1.7	31.0–35.0	8–28	<0.53	6.0–6.4	<0.1	<0.15	<0.15	<4	1.55–1.64	43–54	n/a	n/a	>23
3.9	>1.7	>35.0	<8	<0.53	6.4–6.7	<0.1	<0.15	<0.15	<4	>1.64	<43	n/a	n/a	>23

* References: a, Keck and Sears, 1987; Sears et al., 1991; b, Sears et al., 1991; c, Scott and Jones, 1990; d, McSween, 1977; e, Greenwood and Franchi, 2004; f, Bartoschewitz et al., 2010; g, Bonal et al., 2007; h, Chizmadia et al., 2002; i, Cloutis et al., 2012.

Table 7
Comparison of attributed petrographic types for CO chondrites.

CO3	Find/fall	McSween (1977)	Scott and Jones (1990)	Sears et al. (1991)	Chizmadia et al. (2002)	Bonal et al. (2007)	Present study
ALHA77307	Find	–	3.0	3.1	3.0	3.03	**3.0**
Colony	Find	I	3.0	3.0	3.0	3.1	**3.0**
Kainsaz	Fall	I	3.1	3.2	3.2	3.6	**3.2**
Felix	Fall	II	3.2	3.4	3.3	>3.6(1)	**3.4**
Ornans	Fall	II	3.3	3.4	3.4	>3.6(3)	**3.4**
Lance	Fall	II	3.4	3.4	3.5	>3.6(2)	**3.4**
Warrenton	Fall	III	3.6	3.6	3.7	⩾3.7(1)	**3.6**
Isna	Find	III	3.7	3.7	3.8	⩾3.7(2)	**3.7**

whether igneous, sedimentary, or metamorphic. Furthermore, since they are the products of a differentiated planet, they are, comparatively speaking, compositionally simple. Chondrites are essentially solar in composition and as a result they contain over 200 minerals. They were produced by a process we cannot observe on the Earth today. Volatile elements, including water and organic compounds, are of especially uncertain origin, history, mobility, and distribution. Sometimes there is even uncertainty as to whether processes occurred in the nebula (i.e. via gas–solid reactions) or on the parent body (which is normally assumed to mean solid–solid or solid–liquid reactions, but parent body gas phase reactions cannot be ruled out). The variety and complexity of reactions is large and even well-known chronometers, for instance, have to be applied with caution since they are sensitive to environment and local chemistry and are usually model-dependent or interpretation dependent. The number of secondary events experienced by meteorites is large and complex; aqueous alteration, metamorphism, shock, brecciation, regolith working, and even injection of presolar material, and it is often unclear how a particular phase of lithology was produced or of the relative timing of these different events. Thus conclusions based on one technique, or one phase, and not supported by independent observations should be viewed with caution.

I recommend the subdivision parameters described in Table 6 for the CO chondrites, which is essentially an updated version of the proposal by Scott and Jones (1990) and Sears et al. (1991). This results in the assignments for the well-known CO chondrites shown in Table 7. This is the best summary of what is known about the relative metamorphism experienced by these meteorites and it is practically useful in that none of the assignments are limits. It does have to be borne in mind, as discussed above, that this does not imply that the metamorphic history of all chondrite classes is the same.

4.4.5. The petrographic type of DOM and MIL

Based on petrographic and mineralogical observations the Antarctic Meteorite Newsletter assigned both of the present meteorites were described as petrologic type 3.2. This petrologic type has a TL sensitivity for peak 1 of 0.030–0.054 (Dhajala = 1) whereas the two 500 mg samples of MIL have TL sensitivities of 0.025 ± 0.005 (MIL07182) and 0.021 ± 0.002 (MIL090019) which puts it squarely in the type 3.1 field. The 50 mg splits have a central mode of about 0.57 which puts it on the 3.2/3.3 boundary. On balance I consider assigning type 3.2 as reasonable.

The Antarctic meteorite Newsletter also assigned a petrologic type 3.2 to the DOM CO chondrites. Three of the five 50 mg splits indicates a petrologic type of 3.4 for this meteorite, with the remaining two indicating type 3.0 or 3.2. One of the 500 mg splits has an extraordinarily low TL sensitivity, suggesting that it was composed of highly unusual material and that assigning a type is probably meaningless. On balance, it is suggested that the DOM CO chondrite is a brecciated meteorite with type 3.4 material mixed with lower types. An overall assignment to type 3.2, as suggested by the newsletter seems appropriate recognizing this heterogeneity.

5. CONCLUSIONS

The 29 fragments of the MIL CO chondrite that were paired in the Antarctic Meteorite Newsletter were analyzed by thermoluminescence techniques which confirmed the pairing and found, by low-type 3 standards, that this meteorite is relatively homogeneous. The meteorite seems to have had a "normal" orbit (perihelion ~1 AU) and a terrestrial age of 450–700 ka, relatively old by Antarctic meteorite standards. This was not true of the five CO chondrites from the Dominion Range examined here which are either not paired, or this meteorite is highly heterogeneous. The natural TL data seem to indicate that while some of the meteorites resemble the MIL meteorites in their perihelion and terrestrial age, some had a small perihelion ($<\sim$0.8 AU) and a terrestrial age of ~100 ka. This suggests that that not all of the DOM CO chondrites are paired.

The induced TL properties of the MIL and DOM CO chondrites examined here are consistent with previously studies of CO chondrites and confirm the petrologic type assignment of 3.2 previously assigned in the Antarctic Meteorite Newsletter.

The assignment of meteorites to petrologic types is discussed, first in general terms and then specific to CO chondrites. It is argued that the best classification schemes describe and do not interpret, that they are not rankings (which will change with every new meteorite discovery), and that they should be broadly based and robust, not needing to be frequently changed. Recent suggestions that we give petrologic types three significant figures or define a system that means most of the meteorites in a given class are limits, are not supported. A detailed analysis of all these ideas and the metamorphism related trends in CO chondrites suggests that the most useful petrologic type definitions are those proposed by Scott and Jones (1990) and Sears et al. (1991), which are essentially in agreement.

A Principle Component Analysis indicates that there are three types of process (Components) that are driving the relationships between metamorphism and the properties of CO chondrites. These are: bulk properties (bulk carbon, inert gases, and albedo at 0.8 μm) which explain 30% of the total variance, phase changes (essentially, TL sensitivity and matrix composition, minor contribution from graphite disordering) which explains 28% of the total variance, and Fe diffusion (molar Fa in olivine and Ni in metal) which accounts for 25% of the total variance. The remaining 17% of the variance was explained by several poorly identified minor factors. This suggests that no single technique stands out as the "best" metamorphism sensor in CO chondrites but that all the available data should be taken into account when evaluating the importance of this particular form of secondary alteration in the history of these types of meteorite.

ACKNOWLEDGEMENTS

I am grateful to Tim Lee and Chris McKay for providing facilities and an exciting research environment at NASA Ames Research Center and I am grateful to Mark Sittloh and his colleagues at the Bay Area Environmental Research Institute for management support. I am also grateful to the Antarctic Meteorite

Working Group for providing the samples and the Meteorite Processing Laboratory at Johnson Space Center for so capably handling the sampling. I am also grateful to Hazel Sears for reviewing and proofing this paper, David Sears for help with the statistical analysis, four anonymous journal reviewers who provided much appreciated reviews (which included the suggestion to include Fig. 7), and Chris Herd for organizing these reviews. Finally, I am pleased to acknowledge the Field Investigations to Enable Solar System Science and Exploration team of NASA's Solar System Exploration and Research Virtual Institute (PI: Jennifer Heldmann) for financial support.

REFERENCES

Akridge D. G., Akridge J. M. C., Batchelor J. D., Benoit P. H., Brewer J., DeHart J. M., Keck B. D., Lu Ji, Meier A., Penrose M., Schneider D. M., Sears D. W. G., Symes S. J. K. and Zhang Yanhon (2004) Photomosaics of the cathodoluminescence of 60 sections of meteorites and lunar samples. *J. Geophys. Res.* **109** (E7), CiteID E07S03.

Bartoschewitz R., Ott U., Franke Luitgar, Herrmann S., Yamamoto Y., Nagao K., Bilet M. and Grau T. (2010) Noble gas record and cosmic-ray exposure history of the new CO3 chondrite Moss-Comparison with Lancé and other CO chondrite falls. *Meteorit. Planet. Sci.* **45**, 1380–1391.

Benoit P. H. and Sears D. W. G. (1993) Breakup and structure of an H-chondrite parent body: the H-chondrite flux over the last million years. *Icarus* **101**, 188–200.

Benoit P. H. and Sears D. W. G. (1994) A recent meteorite fall in Antarctic with an unusual orbital history. *Earth Planet. Sci. Lett.* **120**, 463–471.

Benoit P. H. and Sears D. W. G. (1997) Orbits of meteorites from Natural TL. *Icarus* **125**, 281–287.

Benoit P. H., Sears D. W. G. and McKeever S. W. S. (1991) The natural thermoluminescence of meteorites – II. Meteorite orbits and orbital evolution. *Icarus* **94**, 311–325.

Benoit P. H., Sears D. W. G. and McKeever S. W. S. (1993) Natural thermoluminescence and terrestrial ages of meteorites from a variety of temperature regimes. *Radiat. Detect. Dosimet.* **47**, 669–674.

Benoit P. H., Hartmetz C. P., Batchelor D. J., Symes S. J. K. and Sears D. W. G. (2001) The induced thermoluminescence and thermal history of plagioclase feldspars. *Am. Mineral.* **76**, 780–789.

Bland P. A., Zolensky M. E., Benediz G. K. and Sephton M. A. (2006) Weathering of chondritic meteorites. In *Meteorites and the Early Solar System II* (eds. D. S. Lauretta and H. Y. McSween, Jr.). University of Arizona Press, Tucson. 943 pp., pp. 853–867.

Bonal L., Bourot-Denise M., Quirico E., Montagnac G. and Lewin E. (2007) Organic matter and metamorphic history of CO chondrites. *Geochim. Cosmochim. Acta* **71**, 1605–1623.

Brearley A. J. and Jones R. H. (1998) Chondritic meteorites. In *Planetary Materials, Reviews in Mineralogy*, vol. 36 (ed. J. J. Papike). Mineralogical Society of America, Washington, DC (Chapter 3).

Cassidy W., Harvey R., Schutt J., Delisle G. and Yanai K. (1992) The meteorite collection sites of Antarctica. *Meteoritics* **27**, 490–525.

Chizmadia L. J., Rubin A. E. and Wasson J. T. (2002) Mineralogy and petrology of amoeboid olivine inclusions in CO3 chondrites: relationship to parent-body aqueous alteration. *Meteorit. Planet. Sci.* **37**, 1781–1796.

Chung D. D. L., Dresselhaus G. and Dresselhaus M. S. (1977) Intralayer crystal structure and order-disorder transformation using electron diffraction techniques. *Mater. Sci. Eng.* **31**, 107–114.

Clayton R. N. and Mayeda T. K. (1999) Oxygen isotope studies of carbonaceous chondrites. *Geochim. Cosmochim. Acta* **63**, 2089–2104.

Clayton R. N., Mayeda T. K., Goswami J. N. and Olsen E. J. (1991) Oxygen isotopes studies of ordinary chondrites. *Geochim. Cosmochim. Acta* **55**, 2317–2337.

Cloutis E. A., Hudon P., Hiroi T., Gaffey M. J. and Mann P. (2012) Spectral reflectance properties of carbonaceous chondrites – 5: CO chondrites. *Icarus* **220**(2012), 466–486.

Dodd R. T. (1972) *Calcium in Chondritic Olivine*. Geological Society of America Memoirs 132, pp. 651–660.

Dodd R. T., Van Schmus W. R. and Koffman D. M. (1967) A survey of the unequilibrated ordinary chondrites. *Geochim. Cosmochim. Acta* **31**, 921–951.

Engel M. and Macho S. A. (1993) *Organic Geochemistry: Principles and Applications*. Springer, p. 861.

Garlick G. F. J. (1949) *Luminescent Materials*. Clarendon Press, p. 254.

Gietzen K. M., Lacy C. H. S., Ostrowski D. R. and Sears D. W. G. (2012) IRTF observations of S complex and other asteroids: implications for surface compositions, the presence of clinopyroxenes, and their relationship to meteorites. *Meteorit. Planet. Sci.* **47**, 1789–1808.

Greenwood R. C. and Franchi I. A. (2004) Alteration and metamorphism of CO3 chondrites: evidence from oxygen and carbon isotopes. *Meteorit. Planet. Sci.* **39**, 1823–1838.

Grossman J. N. and Brearley A. J. (2005) The onset of metamorphism in ordinary and carbonaceous chondrites. *Meteorit. Planet. Sci.* **40**, 87–122.

Guimon R. K., Symes S. P., Sears D. W. G. and Benoit P. H. (1995) Chemical and physical studies of type 3 chondrites XII: the metamorphic history of CV chondrites and their components. *Meteoritics* **30**, 707–714.

Hasan F. A., Haq M. and Sears D.W.G. (1987) Natural thermoluminescence levels in meteorites, I: 23 meteorites of known Al-26 content. In *Proc. 17th Lunar and Planet. Sci. Conf., Part 2, J. Geophys. Res.*, 92. pp. E703–E709.

Hasan F. A., Score R. and Sears D. W. G. (1989) The natural thermoluminescence survey of Antarctic meteorites – a discussion of methods of reporting natural TL data. *Lunar Planet. Sci.* **XX**, 383–384.

Huss G. R., Keil K. and Taylor G. J. (1981) The matrices of unequilibrated ordinary chondrites: implications for the origin and history of chondrites. *Geochim. Cosmochim. Acta* **45**, 33–51.

Jarosewich E. (1990) Chemical analyses of meteorites: a compilation of stony and iron meteorite analyses. *Meteoritics* **25**, 323–337.

Jull A. J. T., Cloudt S. and Cielaszyk E. (1998) ^{14}C terrestrial ages of meteorites from Victoria Land, Antarctica, and the infall rates of meteorites. In *Geological Society, London, Special Publications*, vol. 140, pp. 75–91. Geological Society, London, Special Publications. http://dx.doi.org/10.1144/GSL.SP.1998.140.01.08.

Kallemeyn G. W. and Wasson J. T. (1981) The compositional classification of chondrites. I – the carbonaceous chondrite groups. *Geochim. Cosmochim. Acta* **45**, 1217–1230.

Keck B. D. and Sears D. W. G. (1987) Chemical and physical studies of type 3 chondrites – VIII: thermoluminescence and metamorphism in the CO chondrites. *Geochim. Cosmochim. Acta* **51**, 3013–3022.

McKeever S. W. S. (1980) The analysis of thermoluminescence glow-curves from meteorites. *Mod. Geol.* **7**, 105–114.

McNaughton N. J., Borthwick J., Fallick A. E. and Pillinger C. T. (1981) Deuterium/hydrogen ratios in unequilibrated ordinary chondrites. *Nature* **294**, 639–641.

McSween, Jr., H. Y. (1977) Carbonaceous chondrites of the Ornans type: a metamorphic sequence. *Geochim. Cosmochim. Acta* **41**, 477–491.

Mc.Sween, Jr., H. Y. (1979) Are carbonaceous chondrites primitive or processed? A review. *J. Geophys. Space Phys.* **17**, 1059–1078.

Melcher C. M. (1981a) Thermoluminescence of meteorites and their orbits. *Earth Planet. Sci. Lett.* **52**, 39–54.

Melcher C. M. (1981b) Thermoluminescence of meteorites and their terrestrial ages. *Geochim. Cosmochim. Acta* **45**, 615–626.

Nishiizumi K., Arnold J. R., Elmore D., Ferraro R. D., Gove H. E., Finkel R. C., Beukens R. P., Chang K. H. and Kilius L. R. (1979) Measurements of ^{36}Cl in Antarctic meteorites and Antarctic ice using a Van de Graaff accelerator. *Earth Planet. Sci. Lett.* **45**, 285–292.

Russell S. S., Huss G. R., Fahey A. J., Greenwood R. C., Hutchison R. and Wasserburg G. J. (1998) An isotopic and petrologic study of calcium–aluminum-rich inclusions from CO3 meteorites. *Geochim. Cosmochim. Acta* **62**, 689–714.

Schultz L. and Franke L. (2004) Helium, neon, and argon in meteorites: a data collection. *Meteorit. Planet. Sci.* **39**(11), 1889–1890.

Scott E. R. D. and Jones R. H. (1990) Disentangling nebular and asteroidal features of CO3 carbonaceous chondrite meteorites. *Geochim. Cosmochim. Acta* **54**, 2485–2502.

Scott E. R. D. and Taylor G. J. (1983) Chondrules and other components in C, O, and E chondrites: similarities in their properties and origins. Lunar and Planetary Science Conference, 14th. *J. Geophys. Res.*(Suppl. 88), B275–B286.

Sears D. W. (1975) Temperature gradients in meteorites produced by heating during atmospheric passage. *Mod. Geol.* **5**, 155–164.

Sears D. W. G. and Weeks K. S. (1983) Chemical and physical studies of type 3 chondrites – II: thermoluminescence of sixteen type 3 ordinary chondrites and relationships with oxygen isotopes. In: *Proc. 14th Lunar Planet. Sci. Conf., part 1, J. Geophys. Res.*, 88. pp. B301–B311.

Sears D. W. G., Grossman J. N., Melcher C. L., Ross L. M. and Mills A. A. (1980) Measuring metamorphic history of unequilibrated ordinary chondrites. *Nature* **287**, 791–795.

Sears D. W. G., Batchelor J. D., Lu J. and Keck B. D. (1991) Metamorphism of CO and CO like chondrites and comparisons with type 3 ordinary chondrites. *Proc. NIPR Symp. Antarct. Meteorites* **4**, 319–343.

Sears D. W. G., Yozzo J. and Ragland C. (2011) The natural thermoluminescence of Antarctic meteorites and their terrestrial ages and orbits: a 2010 update. *Meteorit. Planet. Sci.* **46**, 79–91.

Sears D. W. G. (2013) The metamorphic history of two major new finds of Antarctic CO chondrites (DOM 08004 and MIL 07531) determined from thermoluminescence data. In *44th Lunar and Planetary Science Conference, held March 18–22, 2013 in The Woodlands, Texas*. LPI Contribution No. 1719, p.2333.

Sears D. W. G., Ninagawa K. and Singhvi A. K. (2013) Luminescence studies of extraterrestrial materials: insights into their recent radiation and thermal histories and into their metamorphic history. *Chem. Erde* **73**, 1–37.

Van Schmus W. R. and Wood J. A. (1967) A chemical-petrologic classification for the chondritic meteorites. *Geochim. Cosmochim. Acta* **31**, 747–765.

Wiik H. B. (1969) On regular discontinuities in the composition of meteorites. *Comment. Phys. Math.* **34**, 135–145.

Wood J. A. (1962) Metamorphism in chondrites. *Geochim. Cosmochim. Acta* **26**, 739–749.

Zolensky M., Barrett R. and Browning L. (1993) Mineralogy and composition of matrix and chondrule rims in carbonaceous chondrites. *Geochim. Cosmochim. Acta* **57**, 3123–3148.

Associate editor: Chris Herd